Glassy Wasteforms for Nuclear Waste Immobilization

MICHAEL I. OJOVAN and WILLIAM E. LEE

Glassy wasteforms currently being used for high-level radioactive waste (HLW) as well as for low- and intermediate-level radioactive waste (LILW) immobilization are discussed and their most important parameters are examined, along with a brief description of waste vitrification technology currently used worldwide. Recent developments in advanced nuclear wasteforms are described such as polyphase glass composite materials (GCMs) with higher versatility and waste loading. Aqueous performance of glassy materials is analyzed with a detailed analysis of the role of ion exchange and hydrolysis, and performance of irradiated glasses.

DOI: 10.1007/s11661-010-0525-7

I. INTRODUCTION

THE choice of wasteform to use for nuclear waste immobilization is a difficult decision, and durability is not the sole criterion. In any immobilization process where radioactive materials are used, the process and operational conditions can become complicated, particularly if operated remotely and equipment maintenance is required. Therefore, priority is given to reliable, simple, rugged technologies and equipment, which may have advantages over complex or sensitive equipment. A variety of matrix materials and techniques is available for immobilization. The choice of the immobilization technology depends on the physical and chemical nature of the waste and the acceptance criteria for the long-term storage and disposal facility to which the waste will be consigned. A host of regulatory, process, and product requirements has led to the investigation and adoption of a variety of matrices and technologies for waste immobilization. The main immobilization technologies that are available commercially and have been demonstrated to be viable are cementation, bituminization, and vitrification.[1] Vitrification is a particularly attractive immobilization route because of the high chemical durability of the glassy product. This characteristic was used by industry for centuries. The chemical resistance of glass can allow it to remain in a corrosive environment for many thousands and even millions of years. In most countries, High-level radioactive waste (HLW) has been incorporated into alkali borosilicate or phosphate vitreous waste forms for many years, and vitrification is an established technology. Large streams of low- and intermediate-level radioactive waste (LILW) are planned to be vitrified in the United States, South Korea, and Russia. Vitreous waste forms represent one end of the spectrum of the HLW waste forms shown in Table I.[2,3]

At the other end of the spectrum shown in Table I, the use of predominantly crystalline ceramic wasteforms (ceramication) has also been proposed including single-phase ceramics such as zircon to accommodate a limited range of active species such as Pu and multiphase systems such as Synroc to accommodate a broader range of active species.[4] To date, these systems have not been used extensively to immobilize active waste. Recently, however, there has been a trend to systems intermediate between the "completely" glassy or crystalline materials.[5] An illustration of nuclear waste forms used and developed for industrial application is given in Figure 1.[6] Typically, nondurable crystals are Na_2SO_4, Na_2MoO_4 $2H_2O$, $CaMoO_4$, NaF, and NaCl, whereas durable crystals include $BaAl_2Ti_6O_7$, $CaZrTi_2O_7$, $CaTiO_3$, and TiO_2.

GCMs include the following: (1) glass ceramics in which a glassy waste form is crystallized in a separate heat treatment[7,78]; (2) GCMs in which, *e.g.*, a refractory waste is encapsulated in glass such as hot-pressed lead silicate glass matrix encapsulating up to 30 vol pct of $La_2Zr_2O_7$ pyrochlore crystals to immobilize minor actinides[9]; (3) GCM formed by pressureless sintering of spent clinoptiloite from aqueous waste processing[10]; (4) some difficult wastes such as the French HLW U/Mo-containing materials immobilized in a GCM termed U-Mo glass formed by cold crucible melting that partly crystallize on cooling[11]; (5) yellow phase containing wastes are immobilized in Russia in a yellow phase GCM containing up to 15 vol pct of sulfates, chlorides, and molybdates[12]; and (6) GCM that immobilizes ashes from incineration of solid radioactive wastes.[13] Note that alkali-rich wastes at the Hanford site are also immobilized in glassy wasteforms with high crystal contents that characterize them as GCMs.[14]

GCMs may be used to immobilize long-lived radionuclides (such as actinide species) by incorporating them into the more durable crystalline phases, whereas the short-lived radionuclides may be accommodated in the less durable vitreous phase. Historically, the crystallization of vitreous waste forms has always been regarded as undesirable, as it has the potential to alter the

MICHAEL I. OJOVAN, Assistant Professor, is with the Department of Materials Science and Engineering, Immobilisation Science Laboratory, University of Sheffield, Sheffield, S1 3JD, United Kingdom. Contact e-mail: M.Ojovan@sheffield.ac.uk WILLIAM E. LEE, Professor, is with the Department of Materials, Imperial College London, London SW7 2AZ, United Kingdom.

Manuscript submitted May 12, 2010.
Article published online November 17, 2010

Table I. Classification of Types of Glass/Ceramic Waste Forms

Glasses	Glass Composite Materials (GCMs)	Crystalline Ceramics
Magnox, UK	Glass ceramics	Single phase
Defense Waste Processing Facility and West Valley Demonstration Project, Savannah River, SC	Crystal waste encapsulated in glass matrix	Multiphase (*e.g.*, Synroc*)
Alumina phosphate, Russia		

*Synroc consists of titanates hollandite ($BaAl_2Ti_6O_{16}$), zirconolite ($CaZrTi_2O_7$), perovskite ($CaTiO_3$), and TiO_2. The hollandite mainly fixes the fission products and some process chemicals, whereas actinides and rare earth elements are bound in zirconolite and perovskite.

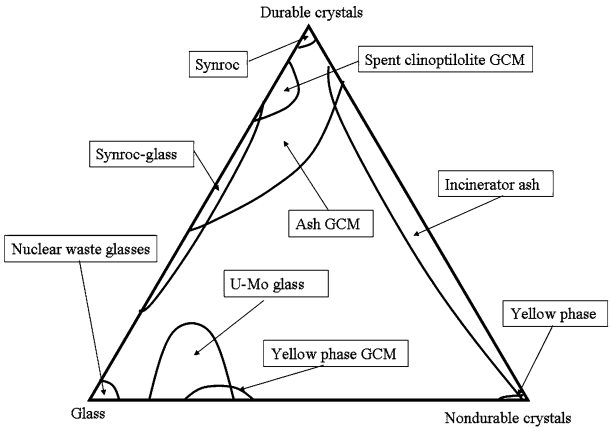

Fig. 1—Phase composition of nuclear waste forms.

composition (and hence, durability) of the remaining continuous glass phase, which would (eventually) come into contact with water. However, there has been a recent trend toward higher crystallinity in ostensibly vitreous wasteforms so that they are more correctly termed GCMs. This is particularly apparent in the development of hosts for more difficult waste or where acceptable durability can be demonstrated even where significant quantities of crystals (arising from higher waste loadings) are present, such as the high sodium Hanford wastes. Acceptable durability will result if the active species are locked into the crystal phases that are encapsulated in a durable, low-activity glass matrix. The GCM option is being considered in many countries including Australia, France, Russia, South Korea, the United Kingdom, and the United States. The processing, compositions, phase assemblages, and microstructures of GCMs may be tailored to achieve the necessary material properties.

II. STABILITY OF GLASSES

Glasses as amorphous materials are among the most abundant materials on the earth. Moreover, glasses are among the most ancient of all materials used by humans. The geological glass obsidian was used first by humans thousands of years ago to form objects including knives, arrow tips, and jewelry. Human-made glass objects were first reported in the Mesopotamian region as early as 4500 BC, and glass objects dating as old as 3000 BC have been found in Egypt. These glasses have compositions similar to those of modern soda-lime-silicate glass as soda ash from fires, limestone from seashells, and silica sand from the beaches were readily available. Current human-made glasses include a large variety of materials from window panels and cookware to aerospace windows and bulk metallic glasses, as well as nuclear waste glassy materials.[12,15–17]

Glasses have an internal structure made of a well-developed, topologically disordered, three-dimensional (3-D) network of interconnected microscopic structural blocks. Glasses are formed typically on rapid cooling of melts to avoid crystallization, because little time is allowed for the ordering processes. Whether a crystalline or amorphous solid forms on cooling depends also on the ease with which a random atomic structure in the liquid can transform to an ordered state. Most known glassy materials are characterized by atomic or molecular structures that are relatively complex and become ordered only with some difficulty. Therefore, it has long been assumed that the glassy state is characteristic of special glass-forming or network materials such as covalent substances that exhibit a high degree of structure organization at length scales corresponding to several atomic separations. However, after the discovery of metallic glasses, it was realized that almost any substance, if cooled sufficiently fast, could be obtained in the glassy state.[18,19]

Glasses are solid amorphous materials with a topologically disordered structure of interconnected structural blocks, which in, *e.g.*, silicate glasses are SiO_4 tetrahedra. After heating, glasses continuously change most of their properties to those of a liquid-like state in contrast to crystals where such changes occur abruptly at a fixed temperature (the melting point). The solid-like behavior of amorphous materials at low temperatures is separated from liquid-like behavior at high temperatures by the glass transition temperature T_g. The glass transition is a kinetically controlled, fairly sharp change in derivative properties such as thermal expansion coefficient or specific heat. T_g depends on the rate of cooling, although empirically it can be calculated roughly from Kauzmann's relation

$$T_g \approx (2/3)T_L \quad [1]$$

where T_L is the liquidus temperature at which a phase diagram shows a crystal-free melt. The liquid–glass transition has been considered as a second-order phase

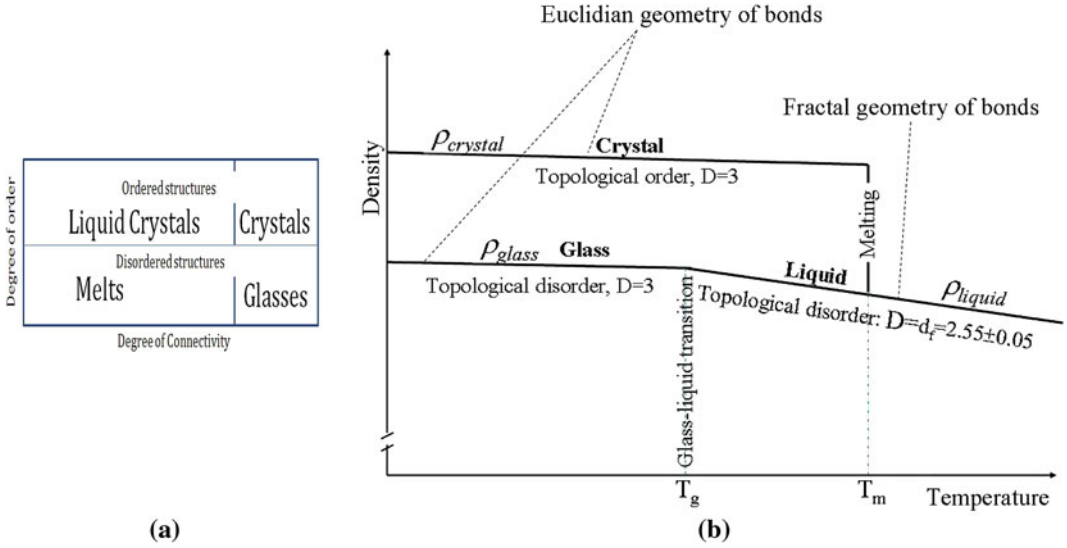

Fig. 2—(*a*) State of crystal and amorphous materials as a function of connectivity. (*b*) Temperature behavior of density and geometry of bonds.

transition in which a supercooled melt yields, on cooling, a glassy structure and properties similar to those of crystalline materials, *e.g.*, of an isotropic solid material.[20]

Amorphous oxide materials have an internal structure made of a 3-D network of interconnected structural blocks where each broken bond is treated as an elementary configurational excitation—configuron.[21,22] Whether a material is liquid or solid depends primarily on the connectivity between its elementary building blocks so that solids are characterized by a high degree of connectivity, whereas structural blocks in fluids have lower connectivity (Figure 2(a)). Melting of a material can be considered as a percolation via broken bonds,[23] *e.g.*, melting of an amorphous oxide material occurs when the configurons form a percolation cluster.[24,25] T_g depends on quasiequilibrium thermodynamic parameters of the bonds, *e.g.*, on the enthalpy (H_d) and entropy (S_d) of configurons, which can be found from available experimental data on viscosity[24–26]

$$T_g = H_d/[S_d + R \ln[(1 - \theta_c)/\theta_c]] \quad [2]$$

where R is the gas constant. For strong melts such as SiO_2, the percolation threshold in the previous equation $\theta_c = \vartheta_c$, where ϑ_c is the universal Scher-Zallen critical density in the 3-D space $\vartheta_c = 0.15 \pm 0.01$.[24,25] However, for fragile materials, the percolation thresholds are material dependent, and $\theta_c << 1$.[26] The connectivity of a bond lattice is characterized by its geometry and Hausdorff dimension.[27] Configuron motion in the bond network occurs in the form of thermally activated jumps from site to site. If the temperature is much below T_g, the glass network is characterized as an ideal disordered structure that is described by a Euclidean 3-D geometry. The higher the temperature, the larger the clusters made of configurons in the disordered bond network. Finally, at T_g they form a macroscopic so-called percolation cluster, which penetrates the whole volume of the disordered network.[28] Moreover, the formation of the percolation cluster changes the topology of the bond network from 3-D Euclidean below to fractal $D_f = 2.55 \pm 0.05$-dimensional above the percolation threshold.[29] Hence, the glass–liquid transition can be considered as a percolation-type phase transition with formation near the percolation threshold of dynamic fractal structures[30] or twinkling fractal structures.[31] The glass–liquid transition is therefore associated with the reduction of the Hausdorff dimension of bonds from the 3-D Euclidean in the glassy state to the fractal $D_f = 2.55 \pm 0.05$-dimensional in the liquid state.[27,30] Above T_g, amorphous materials have a fractal geometry of bonds and a liquid-like behavior, whereas glasses are amorphous materials below T_g, when they have solid-like behavior and 3-D geometry of bonds alike crystals (Figure 2(b)). Note that the fractal structures formed near the glass transition are dynamic fractal structures.[22,27,31]

The physical and chemical durability of glasses combined with their high tolerance to compositional changes makes glasses irreplaceable when highly toxic wastes such as long-lived and highly radioactive wastes need reliable immobilization for safe long-term storage, transportation, and consequent disposal. Although, compared with crystalline materials of the same composition, glasses are metastable, their relaxation to a thermodynamically stable crystalline structure is impeded kinetically. Relaxation processes in amorphous materials are controlled by viscosity. Maxwell's relaxation time gives the characteristic relaxation time required to attain stabilized parameters

$$\tau_M = \eta/G \quad [3]$$

where G is the shear modulus and η is the viscosity. The higher the viscosity, the longer the relaxation time. Viscosity change is thermally activated, and glass-forming amorphous oxides are characterized by high viscosities under normal conditions,[18] *e.g.*, fused silica has an activation energy of viscosity at low temperature

of $Q_H = 759$ kJ/mol and a shear modulus 31 GPa, which gives relaxation times as long as $\tau_M \sim 10^{98}$ years. This time is incommensurably longer than the lifetime of the universe ($\sim 1.5 \times 10^{10}$ years). Another example to demonstrate that long-term stability of silicate glasses is practical absent of stress relaxation at room temperatures, *e.g.*, a high permanent internal stress is preserved in glass articles made more than 2000 years ago.[32] Moreover, extrapolation of measured data showed that the time necessary for a 0.5 pct decrease in permanent stress is equal to 2.7×10^{11} years for toughened borosilicate glass.[32]

An intriguing question for nuclear waste glasses is whether the irradiation does or does not affect the relaxation processes, *e.g.*, crystallization of an oxide glass. It was found recently that intensive electron irradiation of silicate glasses can cause a significant decrease of viscosity and spinodal decomposition.[33] However, the dose rates required to observe such effects are much higher than those that occur in vitrified nuclear waste.[34,35] Therefore, the metastability of silicate glasses commonly used by various industries is a theoretical rather than a practical question. Oxide glasses are stable longer than any imaginable geological timescale of our universe.

III. GLASSES FOR NUCLEAR WASTE IMMOBILIZATION

Two main glass types are currently used for nuclear waste immobilization: borosilicates and phosphates. The exact compositions of nuclear waste glasses are tailored for easy preparation and melting, avoidance of phase separation and uncontrolled crystallization, and acceptable chemical durability, *e.g.*, leaching resistance. Vitrification can be performed efficiently at temperatures below 1500 K (1227 °C) because of the volatility of the fission products, notably Cs and Ru, so avoiding excess radionuclide volatilization and maintaining viscosities below 10 Pa second to ensure high throughput and controlled pouring into canisters. A more fluid glass is preferred to minimize blending problems. Phase separation on melting is most important for waste streams containing glass-immiscible constituents; however, these can be immobilized in form of isolated and phase separated disperse phase (in GCMs). The leaching resistance of nuclear waste glasses is a paramount criterion as it ensures low release rates for radionuclides on any potential contact with water.

Vitrification involves melting waste materials with glass-forming additives so that the final vitreous product incorporates the waste contaminants in its macrostructure and microstructure. Hazardous waste constituents are immobilized either by direct chemical incorporation into the glass structure or by physical encapsulation. In the former, waste constituents are dissolved in the glass melt; Si, B, and P are included in the glass network on cooling, whereas others such as Cs, K, Na, Li, Ca, Pb, and Mg act as modifiers. Several glass compositions were designed for nuclear waste immobilization; however, few are used in practice.[1,5,8,12] Table II gives compositions of several nuclear waste glasses.

High waste loadings and high chemical durability can be achieved in both borosilicate and aluminophosphate glasses. Moreover, such glasses immobilize well large quantities of actinides; for example, borosilicate glasses can accommodate up to 7.2 mass pct PuO_2.[37] In contrast to borosilicate melts, molten phosphate glasses are highly corrosive to refractory linings; this behavior has limited their application. Currently, this glass is used only in Russia, which has immobilized HLW from nuclear fuel reprocessing in alumina-phosphate glass since 1987.[16]

It should be emphasized that nuclear waste glasses are never completely homogeneous vitreous materials but contain significant amounts of bubbles, foreign inclusions such as refractory oxides, and other immiscible components. Figure 3 shows an example of SEM characterization of stimulant British Magnox Waste glass, which reveals heterogeneities and phase separation characterized by small droplets from 10 to 20 μm sizes, in which subsequent fine segregation on a scale of about 100 nm was observed.[38]

Encapsulation is applied to elements and compounds that have low solubility in the glass melt and do not fit into the glass microstructure either as network formers or modifiers. Immiscible constituents that do not mix easily into the molten glass are typically sulfates, chlorides, and molybdates, as well as noble metals such as Rh and Pd, refractory oxides with high liquidus temperatures such as PuO_2, noble metal oxides, and spinels.

Encapsulation is carried out either by deliberate dispersion of insoluble compounds into the glass melt, immiscible phase separation on cooling, or by sintering

Table II. Compositions of Some Nuclear Waste Glasses, Mass Pct

Plant, Waste, Country	SiO_2	P_2O_5	B_2O_3	Al_2O_3	CaO	MgO	Na_2O	Miscellaneous	Waste Loading
R7/T7, HLW, France	47.2	—	14.9	4.4	4.1	—	10.6	18.8	≤28
DWPF, HLW, United States	49.8	—	8.0	4.0	1.0	1.4	8.7	27.1	≤33
WVP, HLW, UK	47.2	—	16.9	4.8	—	5.3	8.4	17.4	≤25*
PAMELA, HLW, Germany—Belgium	52.7	—	13.2	2.7	4.6	2.2	5.9	18.7	<30
Mayak, HLW, Russia	—	52.0	—	19.0	—	—	21.2	7.8	≤33†
Radon, LILW, Russia	43	—	6.6	3.0	13.7	—	23.9	9.8	<35

*It was demonstrated recently that waste loading can be increased up to 35 pct to 38 pct.[36]
†≤10 for fission products and minor actinide oxides.

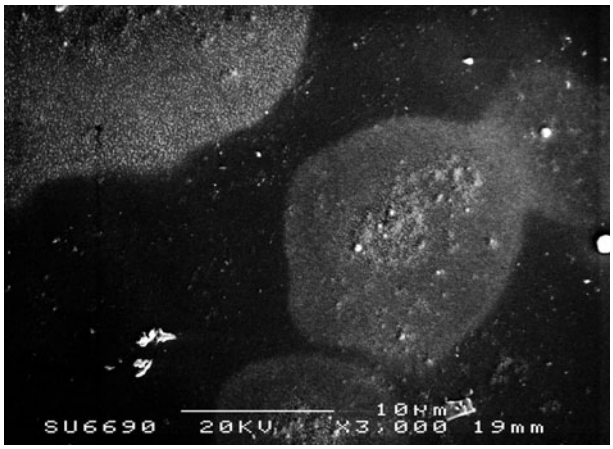

Fig. 3—British Magnox-waste glass secondary electron image.

of glass and waste powders so that the waste form produced is a GCM. However, this requires a more complex melter supplied with a stirrer.

IV. GLASSES FOR HIGH-, LOW-, AND INTERMEDIATE-LEVEL WASTES

Although developed initially for HLW, vitrification is used currently for immobilization of LILW, such as from operation and decommissioning of nuclear power plants.[39,40] Vitrification is one technology that has been chosen to solidify 18,000 tonnes of ore mining tailings at the Fernald, OH plant.[41] Plans are in place to vitrify vast volumes of waste; for example, the vitrification of the low-level radioactive waste at Hanford, WA is expected to produce more than 160,000 m^3 of glass.[42] The U.S. Department of Energy (DOE) plans to vitrify 54 million gallons of mixed radioactive waste stored at its Hanford site in eastern Washington State, which represents 60 pct of the United States' volume of radioactive waste.[43] The world's largest waste vitrification plant (Waste Treatment Project (WTP)) is now under construction at Hanford. Borosilicate glass will be used for immobilization of Hanford's low-activity waste (LAW). The vitrified LAW will be disposed of in a shallow land-burial facility. The proposed disposal system has been shown to retain the radionuclides adequately and prevent contamination of the surrounding environment. Release of radionuclides from the waste form via interaction with water is the prime threat to the environment surrounding the disposal site; the two major dose contributors in Hanford LAW glass that must be retained are ^{99}Tc and ^{129}I.[44] Several glasses were developed to immobilize Hanford low-activity wastes with composition ranges that will meet the performance expectations of the Hanford site burial facility.[44] It is planned that the WTP will vitrify 99 pct of Hanford's waste by 2028. The WTP melter chosen to vitrify HLW is a joule-heated ceramic melter (JHCM). The JHCM has nickel–chromium alloy electrodes that heat the waste and glass-forming additives to ~1450 K (1150 °C). The glass melt is stirred by convection and by bubbler elements, and then poured into carbon steel canisters to cool. Note that the carbon steel canisters are not corrosion resistant and do not present a barrier in an envisaged repository environment. Canisters with vitrified HLW are sealed and decontaminated. It was planned that the vitrified HLW would be disposed of in the Yucca Mountain geological repository; although because of the change in the U.S. government policy, this HLW will need to be stored. Current plans also provide for the vitrified LAW to be stored on site. Moreover, at Hanford, it is planned to use a bulk vitrification process in which liquid waste is mixed with controlled-composition soil in a disposable melter.[43] The process of bulk vitrification involves mixing LAW with Hanford's silica-rich soil and surrounding it with sand and insulation in a large steel box. Electrodes are inserted to vitrify the mixture, and when cooled, the melter, its contents, and the embedded electrodes will be buried as low-level waste (LLW) in an on-site burial ground.

The vitrification of LLW and intermediate-level waste (ILW) was studied intensively in Russia in the middle of 1970s.[12] A number of glass compositions were developed for immobilization of liquid waste containing mainly sodium nitrate. Various boron-containing minerals as well as sandstone were tested as glass-forming additives. Datolite $CaBSiO_4(OH)$ was found to be most suitable fluxing agent. Other systems such as Na_2O (LILW oxides)-2CaO B_2O_3-SiO_2 were studied and glass forming regions, melt viscosity and resistivity, leach rate of sodium (and ^{137}Cs for actual waste), density, radiation stability, and compressive strength were measured. Suitable glass composition areas were established.[12] The most important properties of these glasses are given in Table III.

Loam and bentonite clays were also used as glass-forming additives. Up to 50 pct of either loam clay or bentonite in the batch was substituted for sandstone. This substitution increases the chemical durability of glass and, moreover, such batches containing 20 to 25 wt pct of water form homogeneous pastes, which are stable for long times without segregation and are transportable in pipes over long distances.[12] Sodium nitrate is the major component of both institutional liquid LILW and nuclear power plant (NPP) operational wastes from RBMK (channel type uranium-graphite) reactors. NPP wastes from WWER reactors contain boron, although the major components of this waste are sodium nitrate and sodium tetrahydroxyl borate $NaB(OH)_4$. Thus, there is no need to add boron-containing additives to vitrify WWER waste. Silica, loam, or bentonite clay or their mixtures are suitable as glass-forming additives. WWER waste glasses are in the Na_2O-(Al_2O_3)- B_2O_3-SiO_2 system for which glass-forming regions are well known. Long-term tests of vitrified LILW have been carried out in a shallow ground experimental repository since 1987.[46] These show a low and diminishing leaching rate of radionuclides. Boron-free aluminosilicate glasses in the Na_2O-CaO-Al_2O_3-SiO_2 system for immobilization of institutional and RBMK wastes were produced from waste, sandstone, and loam clay (or bentonite).

Table III. Properties of Vitrified LILW

Properties	Borosilicate Glasses: High Sodium Waste	Borosilicate Glasses: Operational WWER* Waste	GCM Glass Immiscible (High Sulfate) Waste
Waste oxide content, mass pct	30 to 35	35 to 45	30 to 35 and up to 15 vol pct of immiscible waste*
Viscosity, Pa s, at 1500 K (1227 °C)	3.5 to 5.0	2.5 to 4.5	3.0 to 6.0 (for vitreous phase)
Resistivity, Ω m, at 1500 K (1227 °C)	0.03 to 0.05	0.02 to 0.04	0.03 to 0.05†
Density, g/cm^3	2.5 to 2.7	2.4 to 2.6	2.4 to 2.7
Compressive strength, MPa	80 to 100	70 to 85	50 to 70
Normalized Leach Rate, g/(cm^2 day), (28-day IAEA test)			
^{137}Cs	10^{-5} to 10^{-6}	~10^{-5}	10^{-4} to 10^{-5}
^{90}Sr	10^{-6} to 10^{-7}	~10^{-6}	10^{-6} to 10^{-7}
Cr, Mn, Fe, Co, Ni	~10^{-7} to 10^{-8}	~10^{-7}	10^{-7} to 10^{-8}
REE, An	~10^{-8}	~10^{-8}	~10^{-8}
Na	10^{-5} to 10^{-6}	~10^{-5}	10^{-4} to 10^{-5}
B	<10^{-8}	<10^{-8}	≤10^{-8}
SO_4^{2-}	~10^{-6} (when present)	—	10^{-4} to 10^{-5} at content <15 vol pct

*WWER or VVER, water-water energetic reactor, Russian analog of Western PWR, pressurized water reactor.
†For example, "yellow phase."[45]

Some liquid waste streams contain sulfate and chloride ions, which limits the waste oxide content to 5-10 wt pct because of the low sulfate and chloride solubility (~1 pct) in silicate and borosilicate melts. Thus, LILW vitrification becomes inefficient. Excess sulfate–chloride phases segregate as a separate phases floating on the melt surface because of the immiscibility of silicate and sulfate (chloride) melts. The same phenomenon occurs for molybdate- and chromate-containing waste vitrification, where the separate phase is colored and named "yellow phase."[45] Vitrification of this waste can be done by using vigorous melt agitation followed by rapid cooling to the upper annealing temperature to fix the dispersed sulfate–chloride phase into the host borosilicate glass. Sulfate–chloride-containing GCM (see yellow phase GCM in Figure 1) have only a slightly diminished chemical durability compared with sulfate–chloride free aluminosilicate and borosilicate glasses (Table III), which is sufficiently high for them to be used for waste immobilization. GCM produced using a thermochemical technique based on exothermic self-sustaining reactions are also composed of vitreous and crystalline phases, mainly silicates and aluminosilicates.[47]

V. NUCLEAR WASTE VITRIFICATION

Vitrification is most suitable for aqueous radioactive wastes which should be solidified for safer storage and disposal. Waste vitrification is attractive because of the following reasons:

(a) High capability of glass to reliably immobilize a range of elements
(b) Simple production technology adapted from glass manufacture
(c) Small volume of the resulting wasteform
(d) High chemical durability of waste form glasses in contact with natural waters
(e) High tolerance of these glasses to radiation damage.

The high chemical resistance of glass allows it to remain stable in corrosive environments for thousands and even millions of years. Several glasses are found in nature, such as obsidians (volcanic glasses), fulgarites (formed by lightning strikes), tektites found on land in Australasia and associated microtektites from the bottom of the Indian Ocean, moldavites from central Europe, and Libyan Desert glass from western Egypt. Some of these glasses have been in the natural environment for approximately 300 million years with low alteration rates of only tenths of a millimeter per million years.

The excellent durability of vitrified radioactive waste ensures a high degree of environment protection. Waste vitrification gives high waste volume reduction along with simple and cheap disposal facilities. Despite a high initial investment and then operational costs, taking account of transportation and disposal expenses, the overall cost of vitrified radioactive waste is usually lower than alternative options.

The drawbacks of vitrification are its high initial investment cost, high operational cost, and complex technology requiring well-qualified personnel. These reasons made vitrification economically viable when relatively large volumes of radioactive waste with relatively stable composition are available such as HLW or operational radioactive wastes from NPP. Self-sustaining vitrification has no such limitations, in contrast to conventional vitrification technologies; however, this technology is limited to calcined waste streams.[47]

Vitrification technology comprises several stages, starting with evaporation of excess water from liquid radioactive waste, followed by batch preparation,

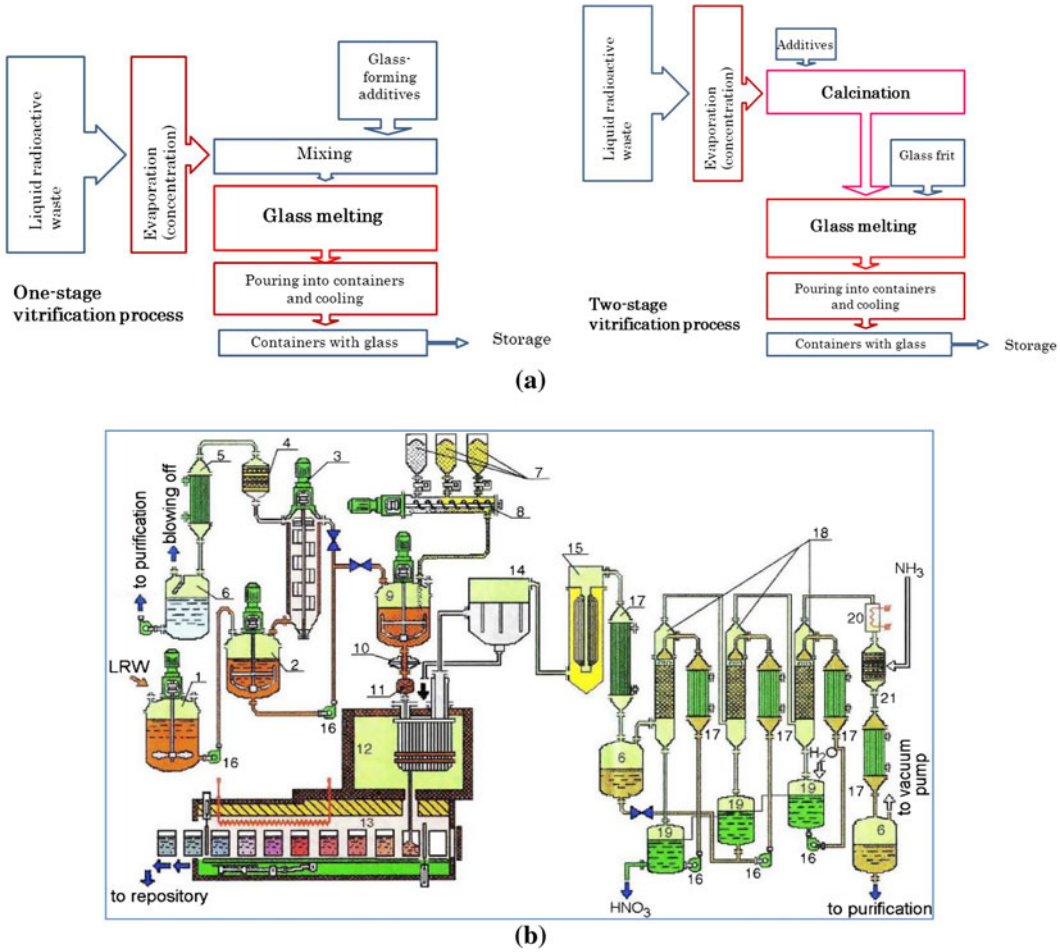

Fig. 4—(*a*) Simplified schematic of a vitrification process. (*b*) Technological flow-sheet diagram of LILW vitrification plant at SIA "Radon." 1—Interim storage tank; 2—concentrate collector; 3—rotary film evaporator; 4, 15—HEPA-filters; 5, 17, 21—heat-exchangers; 6, 19—reservoirs; 7—glass-forming additives hoppers; 8—screw feeder; 9—batch mixer; 10—mechanical activator; 11—peristaltic pump; 12—cold crucible; 13—annealing furnace; 14—sleeve (coarse) filter; 16—pumps; 18—absorption columns; 20—heater. HEPA-filter is high-efficiency particulate air filter and LRW is liquid radioactive waste.[5]

calcination, glass melting, and pouring and cooling of vitrified waste blocks with potentially small amounts of secondary waste (Figure 4).

In a two-stage process, the waste is calcined prior to melting. In the one-stage process, both waste calcination and melting occurs in the melter. Thin film evaporators are typically used, and the remaining salt concentrate is mixed with the necessary additives and, depending on the type of vitrification process, is directed to one or another process apparatus.

In the two-stage vitrification process with separate calcinations, the waste concentrate is fed into the calciner. After calcinations, the required glass-forming additives (usually as a glass frit) together with the calcine are fed into the melter. In both cases, two streams come from the melter: the glass melt containing most of radioactivity and the off gas flow, which contains off gases and aerosols.

In the one-stage vitrification process, glass-forming additives are mixed with concentrated liquid wastes, and so a glass-forming batch is formed (often in the form of a paste). This batch is then fed into the melter where subsequent water evaporation occurs, followed by calcination and glass melting, which occur directly in the melter.

Two types of melters are currently used at waste vitrification plants: JHCMs and induction-heated melters, which can either be hot (induction, hot crucible [IHC]) or cold, *e.g.*, cold crucible melters (CCMs) (Figure 5).

The melt waste glass is poured into containers (canisters) made of stainless steel when immobilizing HLW or carbon steel for vitrified LILW. These may or may not be cooled slowly in an annealing furnace to avoid accumulation of mechanical stresses in the glass. When annealing is not used, cracking occurs resulting in a large surface area being potentially available for attack by water in a repository environment. Despite the higher final surface areas of nonannealed glasses, these are sufficiently durable to ensure a suitable degree of radionuclide retention. Hence, in many cases, annealing is not used in vitrification facilities.

The second stream from the melter goes to the gas purification system, which is usually a complex system

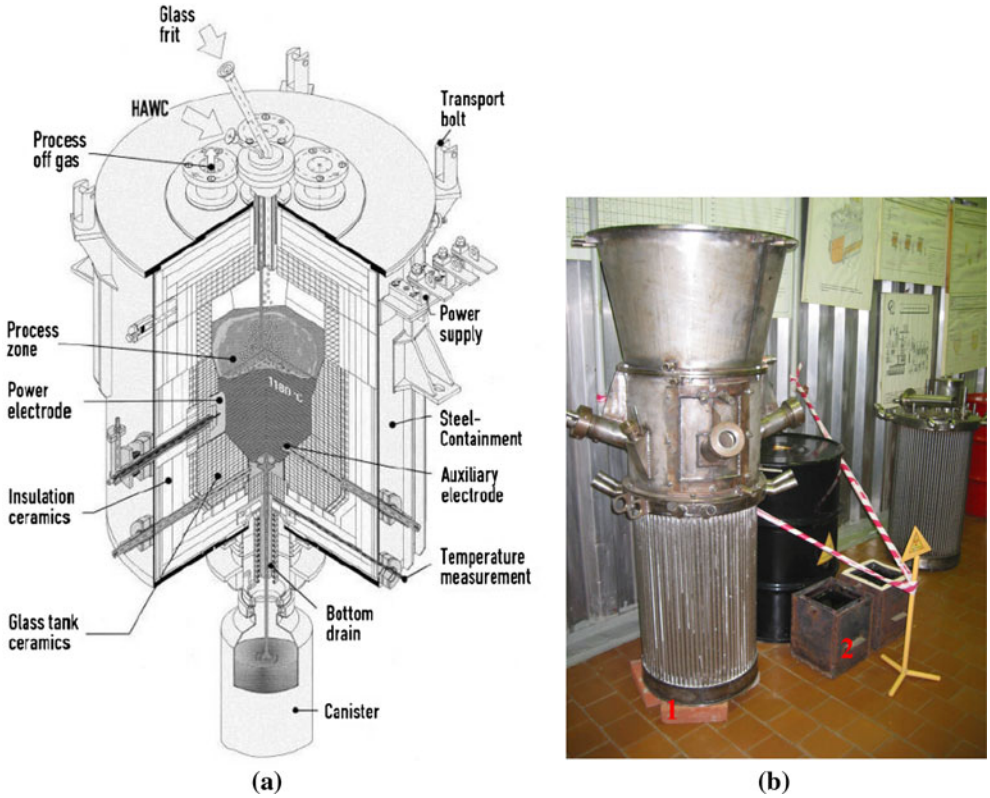

Fig. 5—(*a*) JHCM melter at Nuclear Research Centre (FZK), Karlsruhe, Germany for vitrification of highly active waste concentrate (HAWC).[48] Courtesy S. Weisenburger, Forschungszentrum Karlsruhe. (*b*) A view of a CCM (1) and rectangular carbon steel containers (2) used at Moscow SIA "Radon" for vitrification of LILW.[13]

that removes from the off gas not only radionuclide but also chemical contaminants. Operation of this purification system leads to generation of a small amount of secondary waste. For example, the distribution of beta gross activity at PAMELA waste vitrification plant was >99.88 pct in waste glass and the rest in secondary waste, *e.g.*, <0.1 pct in intermediate-level waste, <0.01 pct in cold waste, and <0.01 pct in off gas.[49] Table IV summarizes data on radioactive waste vitrification facilities.

VI. DURABILITY OF GLASSY WASTEFORMS

The reliability of radionuclide immobilization is characterized by the rate at which radionuclides can be released from the wasteform during long-term storage. As the most plausible path for reintroduction of radioactivity into the biosphere is *via* water, the most important parameters that characterize the ability of glass to hold on to the active species are the leach rates. The leaching behavior of wasteforms containing different amounts of waste radionuclides is compared using the normalized leaching rates NR_i for each i^{th} nuclide expressed in g/cm^2 day and the normalized mass losses NL_i, expressed in g/cm^2. These are determined measuring the concentrations c_i (g/l) of inactive constituents or activities a_i (Bq/L) of radionuclides in the water solution in contact with the wasteform after a time interval Δt expressed in days. The mass fraction of a given nuclide i in a wasteform is defined as

$$f_i = w_i/w_0 \quad [4]$$

where w_i is the mass of nuclide in the wasteform (g) and w_0 is the mass of the wasteform (g). The specific activity of a given radionuclide in a wasteform q_i (Bq/g) is defined as

$$q_i = A_i/w_0 \quad [5]$$

where A_i is the radioactivity of radionuclides in the wasteform (Bq). The normalized leaching rate of non-radioactive nuclides NR_i (g/cm^{2}day) is calculated using the expression

$$NR_i = c_i V/f_i S\Delta t \quad [6]$$

where S is the surface area of the wasteform in contact with the water (cm^2), V is the solution volume (l), and Δt is the test duration in days. The normalized leach rate of radioactive nuclides NR_i (g/cm^{2}day) is calculated using the expression

$$NR_i = a_i V/q_i S\Delta t \quad [7]$$

where a_i (Bq/l) is the specific radioactivity of the solution. Normalized mass losses NL_i (g/cm^2 day) are

Table IV. Operational Data of Vitrification Programs

Facility	Waste Type	Melting Process	Operational Period	Performance
R7/T7, La Hague, France	HLW	IHC	Since 1989/1992	6811 tonnes (237.9 10^6 Ci in 17206 canisters) to 2009
AVM, Marcoule, France	HLW	IHC	Since 1978	857.5 tonnes in 2412 canisters
R7, La Hague, France	HLW	CCM	Since 2003	GCM: U-Mo glass
WVP, Sellafield, UK	HLW	IHC	Since 1991	>5000 canisters to 2009
DWPF, Savannah River, SC	HLW	JHCM	Since 1996	5000 tonnes in 2845 canisters to 2009
WVDP, West Valley, NY	HLW	JHCM	Since 1996	~500 tonnes in 275 canisters to 2002
EP-500, Mayak, Russia	HLW	JHCM	Since 1987	~8000 tonnes to 2009 (900 10^6 Ci)
CCM, Mayak, Russia	HLW	CCM	Pilot plant	18 kg/h by phosphate glass
PAMELA, Mol, Belgium	HLW	JHCM	1985–1991	~500 tonnes in 2200 canisters
VEK, Karlsruhe, Germany	HLW	JHCM	2010	~60 m^3 of HLW (24 10^6 Ci), to be completed in 2010
Tokai, Japan	HLW	JHCM	Since 1995	> 100 tonnes in 241 canisters (110 l) to 2007
Radon, Russia	LILW	JHCM	1987 to 1998	10 tonnes
Radon, Russia	LILW	CCM	Since 1999	> 30 tonnes
Radon, Russia	ILW	SSV	2001 to 2002	10 kg/h, incinerator ash
VICHR, Bohunice, Slovakia	HLW	IHC	1997 to 2001, upgrading work to restart operation	1.53 m^3 in 211 canisters
WIP, Trombay, India	HLW	IHPT	Since 2002	18 tonnes to 2010 (110 10^3 Ci)
AVS, Tarapur, India	HLW	IHPT	Since 1985	
WIP, Kalpakkam, India	HLW	JHCM	Under testing & commissioning	
WTP, Hanford, WA	LLW	JHCM	Pilot plant since 1998	~1000 tonnes to 2000
Taejon, Korea	LILW	CCM	Pilot plant, planned 2005	?
Saluggia, Italy	LILW	CCM	Planned	?

IHC, Induction, hot crucible; CCM, cold crucible induction melter, JHCM, Joule heated ceramic melter; IHPT, induction heated pot type melter; SSV, self-sustaining vitrification.

Table V. Standard Tests on Immobilization Reliability

Test	Conditions	Use
ISO 6961, MCC-1	Deionized water. Static. Monolithic specimen. Sample surface to water volume (S/V) usually 10 m^{-1}. Open to atmosphere. Temperature 298 K (25 °C) for ISO test, 313 K (40 °C), 343 K (70 °C), and 363 K (90 °C) for MCC-1 test	For comparison of waste forms.
MCC-2	Deionized water. Temperature 363 K (90 °C). Closed.	Same as MCC-1 but at high temperatures.
PCT (MCC-3)	Product consistency test. Deionized water stirred with glass powder. Various temperatures. Closed.	For durable waste forms to accelerate leaching.
SPFT (MCC-4)	Single pass flow through test. Deionized water. Open to atmosphere.	The most informative test.
VHT	Vapor phase hydration. Monolithic specimen. Closed. High temperatures.	Accelerates alteration product formation.

determined for nonradioactive and radioactive nuclides respectively from

$$NL_i = c_i V / f_i S \quad [8]$$

and correspondingly for radioactive samples

$$NL_i = a_i V / q_i S \quad [9]$$

A set of standard tests to determine the water durability of vitrified waste and other wasteforms was developed at the Materials Characterization Centre (MCC) of the Pacific Northwest National Laboratory, Richland, WA. These MCC tests are now the internationally approved standards used worldwide. The most important tests are given in Table V.[50]

The glass-formulation methodology defines a range of compositions around a reference formula to allow for slight fluctuations in the composition of the waste feed stream. Figure 6 illustrates schematically the effect of additives on leaching rates.[5,15] For example, the addition of Al_2O_3 improves the leach resistance of borosilicate glasses, whereas higher content of alkalis (Li_2O, Na_2O, K_2O) reduces glass durability.

As the cost-saving incentive is to increase the waste loading in a wasteform, the optimal glassy wasteform compositions are tailored as a compromise between waste loading and final glass durability accounting also for processing parameters on vitrification.[17] Table VI gives typical data on the parameters of HLW borosilicate and phosphate glasses.[5,51]

Vitrified radioactive waste is chemically durable and reliably retains radioactive species. Typical normalized leaching rates NR of vitrified waste forms are below 10^{-5} to 10^{-6} g/cm^2 day. Moreover, as glasses and GCM are highly corrosion resistant, their high nuclide retention is expected to last for many millennia.

VII. LONG-TERM DURABILITY OF NUCLEAR WASTE GLASSES (EFFECT OF TEMPERATURE, pH, AND TIME)

Corrosion durability of vitrified waste is the most important acceptance parameter for disposal.[12,52] Insight into the long-term behavior of nuclear waste glasses is an important issue related to our ability to assess the reliability of nuclear waste immobilization in an envisaged repository environment. The release of radioactive species, which in nuclear waste glasses are invariably cations, can be caused by corrosion of the glass in contact with groundwater. However, the potential contact of water with glass is deferred in actual disposal systems to times after the waste container has been breached. The material selection of the engineered barriers, *e.g.*, canisters depends on each particular country. Stainless steels are considered but also carbon steel, nickel alloys, titanium alloys, and copper may be used. For vitrified HLW containers, which are made of stainless steel, these times are expected to be of the order of many hundreds or even thousands of years. High temperatures and radiation dose rates are likely only for the first few hundred years after HLW vitrification, so that container temperatures will be close to those of the ambient rock by the expected time of contact with groundwater. Moreover, the role of $\beta\gamma$-radiolysis will also become negligible because of low radiation dose rates. Vitrified LILW is almost invariably at the ambient temperature of a repository environment. In addition, this type of waste is expected to be disposed of in near-surface repositories, which are often characterized by near-neutral groundwaters and relatively low host-rock temperatures. Hence, the temperatures of nuclear waste glasses at the times of expected contact with groundwater are likely to be close to those of the surrounding repository environment.

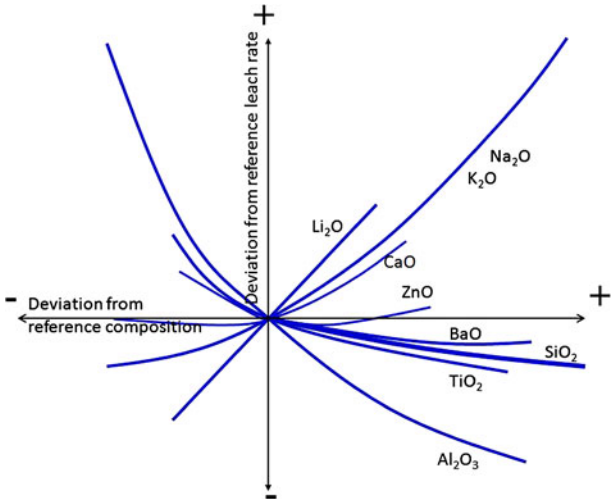

Fig. 6—Glass leach rates as a function of glass composition.

Aqueous corrosion of nuclear waste glasses is a complex process that depends on many parameters such as glass composition and radionuclide content, time, temperature, groundwater chemical composition, and pH. Corrosion of silicate glasses, including nuclear waste borosilicate glasses, involves two major processes: diffusion-controlled ion exchange and glass network hydrolysis.[5,12,18,53–57] Diffusion-controlled ion exchange reactions lead to selective leaching of alkalis and protons entering the silicate structure to produce a hydrated alkali-deficient layer on the glasses. Hydrolysis being a near-surface reaction of hydroxyl ions with the silicate network leads to its destruction, resulting in congruent dissolution of glass constituents and subsequent precipitation of hydrous silica-gel layers as secondary alteration products.

The role of ion exchange in the overall corrosion behavior is important because it is the principal release mechanism when the glass network hydrolysis is suppressed. In dilute near-neutral solutions, ion exchange controls the initial cation release, and at low temperature and pH, it can dominate over hydrolysis for many hundreds of years.[58] Ion exchange involves the interdiffusion and exchange of the cation in the glass with a proton (probably as H_3O^+) from the water. The ion exchange reaction of glass with water can be written as

$$(\equiv \mathrm{Si{-}O{-}A})_{\mathrm{glass}} + \mathrm{H_2O} \leftrightarrow (\equiv \mathrm{Si{-}O{-}H})_{\mathrm{glass}} + \mathrm{A{-}OH} \quad [10]$$

This reaction is controlled by the counter diffusion of protons (probably as H_3O^+) from the water, which replace cations in the glass structure, *e.g.*, cations bounded to nonbridging oxygens (NBO). The rate of

Table VI. Typical Properties of HLW Glasses

Glass	Density (g/cm^3)	Compressive Strength (MPa)	NR, 28th day, in 10^{-6} g/cm^2 day	Thermal Stability,* K (°C)	Damaging Dose,* Gy
Borosilicate	2.7	22 to 54	0.3 (Cs); 0.2 (Sr).	≥ 823 (550)	$>10^9$
Phosphate	2.6	9 to 14	1.1 (Cs); 0.4 (Sr).	≥ 723 (450)	$>10^9$

*The irradiation has a small impact on glasses, and the damaging dose is the absorbed dose above which the radionuclide NR's increase several times, whereas thermal stability is the temperature above which the radionuclide NR's increase $>10^2$ times.

cation release into water via diffusion-controlled ion exchange rx_A is given by[58]

$$rx_A = \rho f_A(\alpha_A D_{0H}/\pi t)^{1/2} 10^{-0.5pH} \exp(-E_{dA}/2RT) \quad [11]$$

where ρ is the glass density, f_A is the mass fraction of the cation A in the glass (Eq. [4]), $\alpha_A = \kappa/C_A(0)$, κ is a constant relating concentration of protons at the glass surface and in the contacting water and $C_A(0)$ is concentration of cations at the glass surface, D_{0H} is the preexponential coefficient in the diffusion coefficient for protons in the glass $D_H = D_{0H} \exp(-E_{dH}/RT)$, E_{dH} is activation energy for diffusion of protons in the glass, t is time and E_{dA} is the activation energy of effective diffusion (kJ/mol). The activation energy for interdiffusion is the sum of the enthalpy of motion of protons or H_3O^+ cations, H_{mH}, and the enthalpy of formation of NBO, H_{NBO}: $E_{dA} = H_{mH} + H_{NBO}$. The average normalized leaching rate caused by the ion exchange processes of cation A, NRx_A (g/cm^2 day), is measured experimentally or it can be found theoretically by calculating the total normalized cation release via ion exchange and dividing it by the leach test duration t (days) resulting in[58]

$$NRx_A = 2\rho(D_A/\pi t)^{1/2} \quad [12]$$

where D_A are the effective diffusion coefficients. The rates of ion exchange with time diminish as the inverse square root of time reflecting the fact that near surface layers of glasses are depleted in cationic species, and deeper and deeper layers are supplying cations for ion exchange reaction. Equation [12] indicates that the ion exchange rate is determined completely by D_A, which depends on the pH of the attacking solution and has an Arrhenius temperature dependence of activation energy E_{dA}. Table VII gives D_A for several silicate glasses tested in near-neutral waters.[58] The second mechanism of silicate glass corrosion—hydrolysis—is represented schematically by the reaction

$$\equiv \text{Si}-\text{O}-\text{Si} \equiv + \text{H}_2\text{O} \leftrightarrow 2(\equiv \text{SiOH}) \quad [13]$$

Hydrolysis results in complete dissolution of the glass network and formation of orthosilicic acid, H_4SiO_4. This process leads to a congruent release of glass constituents into the water. The rate of hydrolysis is calculated using the transition state theory of silicate mineral dissolution[59]

$$rh = k a_{H^+}^{-\eta} [1 - (Q/K)^{\sigma}] \exp(-E_a/RT) \quad [14]$$

where k is the intrinsic rate constant,a_{H^+} is the hydrogen ion activity, η is the pH power law coefficient, E_a is the activation energy and Q the ion-activity product of the rate-controlling reaction, K is the pseudoequilibrium constant of this reaction, and σ is the net reaction order. The rate of release of cations A as a result of hydrolysis is given by

$$rh_A = \rho f_A rh \quad [15]$$

The average normalized leaching rate caused by hydrolysis NRh_A (g/cm^2 day) is measured experimentally or it can be found theoretically by calculating the total normalized cation release via hydrolysis and dividing it by the leach test duration t (days) resulting in

$$NRh_A = \rho rh \quad [16]$$

The affinity term $[1 - (Q/K)^{\sigma}]$ characterizes the decrease in solution aggressiveness with respect to the glass as it becomes increasingly concentrated in dissolved elements and as the ion activity product Q of the reactive species approaches the material solubility product K, *e.g.*, $rh \to 0$, when $Q \to K$. In dilute aqueous systems when $K \ll Q$, the affinity term is simply equal to unity $[1 - (Q/K)^{\sigma}] = 1$. Note that $\eta = 0.5$,[60] and the higher the pH of the attacking water solution the higher the rate of hydrolysis.

Both ion exchange and hydrolysis contribute to aqueous glass corrosion. Because of rapid dissolution of near surface layers, which are generally different from the bulk, there is an additional contribution to leaching termed instantaneous surface dissolution. This is accounted for by an exponential term in the dissolution rate

$$rs_A = n_{sA} k_A \exp(-k_A t) \quad [17]$$

where k_A is the rate of instantaneous dissolution of species i in water (day^{-1}), and n_{sA} is the surface concentration of radionuclides (g · cm^{-2}). The total rate of species released from glass into the water is given by the sum

$$r_A = rs_A + rx_A + rh_A \quad [18]$$

Table VIII summarizes the three most important mechanisms of glass corrosion in nonsaturated aqueous solutions.[61]

Equations [11] and [14] reveal that ion exchange occurs preferentially in acidic and neutral solutions but diminishes quickly with the increase of pH, whereas hydrolysis occurs preferentially in basic solutions but diminishes quickly with the decrease of pH. It is normally considered that for pH < 9 to 10, ion exchange dominates glass corrosion, whereas hydrolysis reactions are significant when the pH exceeds 9.[62,63] In acidic media below pH = 6, the water concentration of protons (or hydronium ions) is high, resulting in a high rate of ion exchange. The role of glass network

Table VII. Effective Diffusion Coefficients in Some Silicates

Glass	Cation A	Temperature, K (°C)	D_A (m^2/s)
USA SM539	B	363 (90)	4×10^{-21}
	Li		7×10^{-21}
	Na		4×10^{-21}
British	Li	313 (40)	1.9×10^{-20}
Magnox-waste	Na		4.4×10^{-20}
Russian O3O-6	Na	295 (22)	2.8×10^{-21}
Russian K-26	Cs	277.5 (4.5)	5×10^{-21}
Russian Bs-10	Cs	284 (11)	1.8×10^{-20}
Quartz artifacts	H	279.6 to 297 (6.6 to 24)	~10^{-25}
Silica glass	H	296 (23)	1.4×10^{-21}

Table VIII. Main Characteristics of Corrosion Mechanisms

Mechanism, Rate Behavior	Instantaneous Surface Dissolution	Ion Exchange	Hydrolysis
Time*	Short-term effect $\propto \exp(-kt)$	Diminishes $\propto t^{-1/2}$	Independent*
Temperature	Arrhenian	Arrhenian, Universal activation energy	Arrhenian, One high activation energy
pH	Dependent	Decreasing $\propto 10^{-0.5pH}$	Increasing $\propto 10^{0.5pH}$
Saturation effects†	Unlikely	Unlikely	Impeded $\propto (1-C_{Si}/C_{Si\ saturation})$
Selectivity	Selective	Selective	Congruent

*Time behavior may be affected by saturation effects.
†Changes in solution chemistry may affect solution pH.

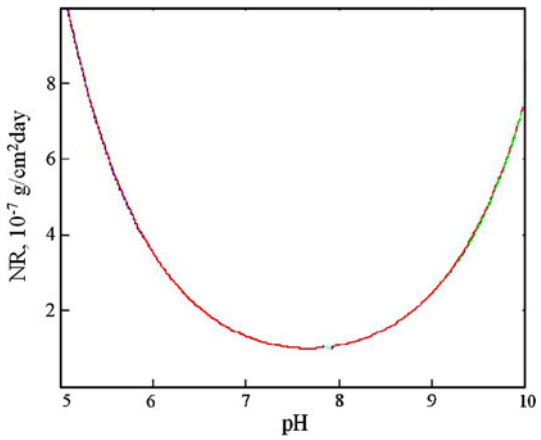

Fig. 7—pH dependence of cesium normalized leaching rate of glass K-26.

dissolution in this process is insignificant, and cation leaching is ion-selective with different leaching curves for different cations. Above pH = 9, the role of ion exchange becomes insignificant because of the high water concentration of hydroxyl ions, and thus, the glass network commences to dissolve rapidly via reaction [13]. In such basic media, the release of cations becomes congruent as destruction of the glass network results in practically complete dissolution of all glass constituents. Note that the hydrolysis reaction [13] becomes impeded if solutions become silica saturated. The pH dependence of corrosion rate has a U-form curve with typical minimal changes in the near-neutral water solutions. Figure 7 illustrates the pH dependence of corrosion rate for borosilicate glass K-26.[61]

Figure 7 indicates the mass release from glass follows simple power laws only below pH = 6 and above pH = 9. In the interval 6 < pH < 9, the dependence is a more complex function with a changing slope when pH changes and with minimal corrosion rates achieved close but not at pH = 7. Because of the time dependence of ion-exchange rates in corroding glasses, the minimum rates drift with time to lower values of pH. Therefore, attempts to model the pH dependences by simple power laws separated at pH = 7 will inevitably result in smaller values of exponent terms m and η. For example, the exponent terms for UK Magnox waste glass based on data from the pH ranges 2 < pH < 7 and 7 < pH < 10 were m = 0.39 for boron, $m = 0.43$ for silicon, and $\eta = 0.43$,[64] which are somewhat smaller than the theoretical value of $m = 0.5$.

The ion-exchange reaction of glass with water leads to a gradual diminution of cation content in the near-surface glass layers. Because of this depletion in the glass near-surface layers over time, the rate of ion exchange diminishes. In contrast, the rate of glass hydrolysis, although small in near-neutral conditions, remains constant. Hence, hydrolysis will eventually dominate, once the near-surface glass layers have become depleted in cations. Depending on glass composition and the conditions of aqueous corrosion, as well as on time, the contribution of the basic mechanisms to the overall corrosion rate can be different. For example, in dilute solutions, ion exchange controls the initial corrosion stage. Moreover, at expected disposal temperatures (below 320 K or several tens of °C), the corrosion of glasses will occur via ion exchange for long periods of time, even in contact with non-silica saturated groundwater, although ion-exchange controls corrosion of glasses over geological timescales when the contacting groundwater is silica saturated and the hydrolytic dissolution of the glass network is impeded.

The time required for silicate glasses to reach the hydrolysis stage in near-neutral solutions depends mainly on glass composition and temperature. Note that we suppose unchanged water parameters, so there is no coupling between water chemistry and the corroding glass. More highly polymerized glasses are hydrolytically decomposed more slowly. Thus, glasses with higher silica contents require longer times before hydrolysis becomes dominant compared with high-sodium-content glasses. The corrosion regimes of silicate glasses should be characterized in terms of time-temperature parameters as the higher the temperature the sooner hydrolysis becomes dominant. This occurs because the activation energy for hydrolysis E_a is significantly higher than the activation energies of diffusive processes E_{dA}. It has been shown that the diffusion-controlled ion exchange stage is dominant up to a time, $\tau(T)$, given by[58,61]

$$\tau(T) = \tau_0 \exp[(2E_a - E_{dA})/RT] \qquad [19]$$

where τ_0 is a preexponential term. The time τ_0 increases with silica concentration approaching the solubility limit when $Q \rightarrow K$, demonstrating that the only important cation release mechanism remains ion exchange in this case. For example, in near-neutral water solutions, UK Magnox-waste glass undergoes incongruent

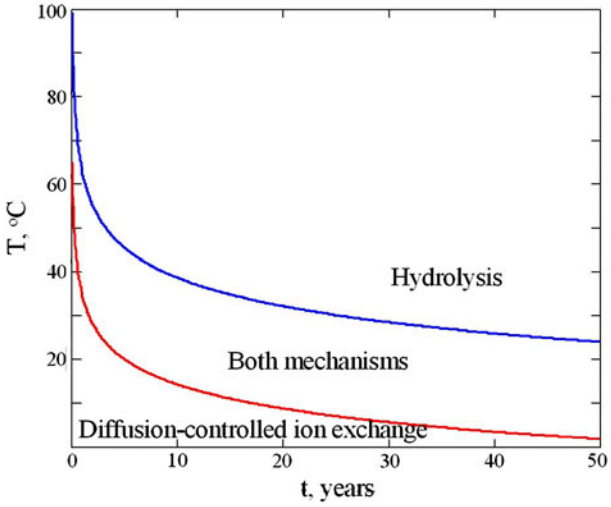

Fig. 8—Corrosion mechanisms for British Magnox-waste glass in deionized water.

Table IX. Transition Times for the Intermediate Stage of Glass Dissolution

Glass	T, K (°C)	τ (T)
British Magnox-waste	363 (90)	>28 days
USA SRL131A, SRL202A	298 (25)	>240 days
Russian Bs-10	284 (11)	3.2 years
Russian K-26	277.5 (4.5)	16.4 years
Roman IF (Archaeological)	287 to 288 (14 to 15)	~1800 years

ion-exchange over a period of 28 days at temperatures as high as 60 °C to 90 °C and an estimate of $\tau(60\ °C) \approx 28$ days, $E_a \approx 60$ kJ mol^{-1} and $E_{di} \approx 36$ kJ mol^{-1}, which enables the tentative identification of the most likely scenarios for corrosion of UK Magnox-waste glass as a function of temperature and time.[58] Figure 8 shows that corrosion in deionized water at a constant temperature immediately after instantaneous surface dissolution begins with a fully controlled ion exchange phase.

As corrosion progresses the impact of hydrolysis becomes significant with comparable contributions from both ion exchange and hydrolytic reactions. Finally, glass corrosion in demonized water is fully controlled by hydrolysis. The characteristic time that indicates the duration of pure ion exchange phase is given by Eq. [19]. Table IX gives characteristic times τ(T) for several glasses corroding in non-Si-saturated near-neutral water solutions. Note that an increase of contacting water pH would decrease characteristic transition times.

VIII. EFFECTS OF SELF-IRRADIATION

Although radiation is not believed to have a significant effect on glass corrosion rates,[65] it can influence glass stability through the formation of corrosive radiolytic products in the contacting water solution, alteration of glass structure, and radiation-enhanced diffusion. For the expected times of water–glass contact ($\geq 10^{3-4}$ years), radiation dose rates are likely to be low so that no intensive radiolysis is expected. Significant alteration of the glass structure is also not expected as the glass is originally amorphous and no more disorder arises from radiation damage than originally is present in the glass structure. The formation of gas bubbles observed in glasses under irradiation as well as redistribution of alkalis is an effect that results from radiation-induced diffusion rather than from alteration of glass structure. Hence, the most important radiation-induced effects in nuclear waste glasses for times of water–glass contact are those that result from radiation-enhanced diffusion. Between the two basic corrosion mechanisms, ion exchange is controlled directly by the diffusion of species in the glass, whereas hydrolysis can be affected only indirectly by radiation-enhanced diffusion. The rate of ion exchange for an irradiated glass is given by Eq. [11], however, with parameters corresponding to an irradiated glass. Because the diffusion coefficients of species are higher compared with nonirradiated glasses, the rates of ion exchange are higher. The higher the absorbed dose and the lower the temperature, the higher the increase in the ion exchange rate.[66] This remains true only until the ion exchange is significant in the corrosion of glasses, *e.g.*, in silica-saturated conditions (when dissolution rh = 0) and at relatively low temperatures and pH < 9. Because of enhanced diffusion coefficients, the selectivity of leaching should be higher compared with unirradiated glasses. In several experiments, the effects of irradiation were observed clearly and characterized. Static leach tests conducted with PNL 76-78 glass immersed in deaerated and demonized water demonstrated the highest pH increase and release rates for Si, B, and Na at the lowest test temperature 323 K (50 °C) and lowest differences at the highest test temperature 363 K (90 °C) for γ-radiation tests at a dose rate 1.75 10^4Gy/hour compared with nonirradiated glass.[67] Moreover, cation releases were most incongruent at 323 K (50 °C) and were almost congruent at 363 K (90 °C).[67,68] Highly incongruent glass dissolution was observed in γ-irradiated in situ tests of waste glasses in Belgian Boom clay; moreover, the glass corrosion mechanism becomes a more diffusion-controlled process in the presence of the radiation field.[69]

The hydrolytic mechanism of corrosion is hardly affected by self-irradiation. Hence, practically no change in corrosion behavior is expected when the dominant mechanism of corrosion is hydrolysis. This conclusion is confirmed by many experiments; for example, unaffected corrosion behavior has recently been found for a Pu-bearing borosilicate glass over a pH interval of 9 to 12 at 353 K to 361 K (80 °C to 88 °C).[70] Leach tests of French SON68 glass in silica-saturated solutions showed that ion-exchange rates are increased after irradiation whereas hydrolysis remained unchanged.[71] Similar effects were observed in irradiated phosphate glasses.[16]

Summarizing the data available leads to the conclusion[72] that the irradiation had a detectable and even significant impact in cases when corrosion occurred via diffusion-controlled ion exchange. These conditions are characterized by relatively low temperatures (≤323 K

[50 °C]), low and medium pH (≤8), relatively high absorbed doses (≥6 10^6 Gy), and for diluted solutions over short corrosion times ($t \leq \tau(T)$). The most important consequences of irradiation in these cases were enhanced leaching rates and incongruency in glass corrosion. In contrast, when hydrolysis controls the glass corrosion, practically no differences were found in the corrosion behavior of nonirradiated and irradiated glasses. These conditions prevail at high temperatures (> 323 K [50 °C]) and high pH of contacting water (>9), as well as long corrosion times in dilute solutions ($t \geq 16\tau(T)$) when, because of cationic depletion of near surface glass layers, ion exchange reactions are diminished.

IX. CONCLUSIONS

Glass is a solid-state material that behaves like a solid crystalline material but has a topologically disordered internal structure. Although, compared with crystalline materials of the same composition, glasses are metastable materials, their relaxation to crystalline structures is kinetically impeded so that practically no crystallization occurs within times that for oxide glasses are longer than the universe lifetime. The physical and chemical durability of glasses combined with their high tolerance to compositional changes makes glasses irreplaceable when highly toxic wastes such as long-lived and highly radioactive wastes need reliable immobilization for safe long-term storage, transportation and consequent disposal. Immobilization of radioactive wastes in glassy materials using vitrification has been used successfully for many years, although novel glassy wasteforms are still being developed, and studies of their properties are performed. Nuclear waste vitrification is attractive because of its flexibility, the large number of elements that can be incorporated in the glass, its high corrosion durability, and the reduced volume of the resulting wasteform. Vitrification is a mature technology and has been used for HLW immobilization for more than 40 years in France, Germany and Belgium, Russia, UK, India, Japan, and the United States. Vitrification involves melting of waste materials with glass-forming additives so that the final vitreous product incorporates the waste contaminants in its macrostructure and microstructure. Hazardous waste constituents are immobilized either by direct incorporation into the glass structure or by encapsulation when the final glassy material can be in form of a GCM. Both borosilicate and phosphate glasses are used currently to immobilize nuclear wastes; moreover, in addition to relatively homogeneous glasses, novel GCMs are used to immobilize problematic waste streams. The spectrum of wastes that are currently vitrified increases from HLW to LILW such as legacy wastes in Hanford, WA and nuclear power plant operational wastes in Russia and Korea. Glassy wasteforms in the form of relatively homogeneous glasses or as GCM incorporating crystalline disperse phases are currently the most reliable hosts used for nuclear waste immobilization.

REFERENCES

1. M.I. Ojovan and W.E. Lee: *An Introduction to Nuclear Waste Immobilization*, Elsevier Science Publishers B.V, Amsterdam, The Netherlands, 2005.
2. W.E. Lee, M.I. Ojovan, M.C. Stennett, and N.C. Hyatt: *Adv. Appl. Ceram.*, 2006, vol. 105 (1), pp. 3–12.
3. W.E. Lee, J. Juoi, M.I. Ojovan, and O.K. Karlina: *Adv. Sci. Tech.*, 2006, vol. 45, pp. 1986–95.
4. I.W. Donald, B.L. Metcalfe, and R.N.J. Taylor: *J. Mater. Sci.*, 1997, vol. 32, pp. 5851–87.
5. M.I. Ojovan and W.E. Lee: *New Developments in Glassy Nuclear Wasteforms*, Nova Science Publishers, New York, NY, 2007.
6. M.I. Ojovan, J.M. Juoi, A.R. Boccaccini, and W.E. Lee: *Mater. Res. Soc. Symp. Proc.*, 2008, vol. 1107, pp. 245–52.
7. P. Loiseau, D. Caurant, O. Majerus, and N. Baffier: *J. Mater. Sci.*, 2003, vol. 38 (843–852), pp. 853–64.
8. D. Caurant, P. Loiseau, O. Majérus, V.A. Chevaldonnet, I. Bardez, and A. Quintas: *Glasses, Glass-Ceramics and Ceramics for Immobilization of Highly Radioactive Nuclear Wastes*, Nova, New York, NY, 2009.
9. A.R. Boccaccini, E. Bernardo, L. Blain, and D.N. Boccaccini: *J. Nucl. Mater.*, 2004, vol. 327, pp. 148–58.
10. J.M. Juoi, M.I. Ojovan, and W.E. Lee: *J. Nucl. Mater.*, 2008, vol. 372, pp. 358–66.
11. N. Henry, P. Deniard, S. Jobic, R. Brec, C. Fillet, F. Bart, A. Grandjean, and O. Pinet: *J. Noncryst. Solids*, 2004, vol. 333, pp. 199–205.
12. I.A. Sobolev, M.I. Ojovan, T.D. Scherbatova, and O.G. Batyukhnova: *Glasses for Radioactive Waste*, Energoatomizdat, Moscow, Russia, 1999.
13. I.A. Sobolev, S.A. Dmitriev, F.A. Lifanov, A.P. Kobelev, S.V. Stefanovsky, and M.I. Ojovan: *Glass Tech.*, 2005, vol. 46, pp. 28–35.
14. D.S. Kim, J.D. Vienna, P.R. Hrma, M.J. Schweiger, J. Matyas, J.V. Crum, D.E. Smith, G.J. Sevigny, W.C. Buchmiller, J.S. Tixier, J.D. Yeager, K.B. Belew: *Development and Testing of ICV Glasses for Hanford LAW*, Richland, SC, 2003.
15. W. Lutze: in *Radioactive Waste Forms for the Future*, W. Lutze and R. Ewing, eds., Elsevier Science Publishers B.V., Amsterdam, The Netherlands, 1988, pp. 1–160.
16. A.A. Vashman, V.E. Samsonov, and A.V. Demin: *Phosphate Glasses with Radioactive Waste*, CNIIatominform, Moscow, Russia, 1997.
17. I.L. Pegg and I. Joseph: in *Hazardous and Radioactive Waste Treatment Technologies Handbook*, C. Ho Oh, ed., CRC Press, Boca Raton, FL, 2001, pp. 1–27.
18. A.K. Varshneya: *Fundamentals of Inorganic Glasses*, Society of Glass Technology, Sheffield, UK, 2006.
19. W.H. Wang, C. Dong, and C.H. Shek: *Mater. Sci. Eng.*, 2004, vol. R (44), pp. 45–89.
20. IUPAC: "Compendium of Chemical Terminology," Royal Society of Chemistry, Cambridge, UK, 1997, pp. 66, 583.
21. C.A. Angell and K.J. Rao: *J. Chem. Phys.*, 1972, vol. 57, pp. 470–81.
22. M.I. Ojovan: *Entropy*, 2008, vol. 10, pp. 334–64.
23. S.Y. Park and D. Stroud: *Phys. Rev. B*, 2003, vol. 67, p. 212202.
24. M.I. Ozhovan: *J. Exp. Theor. Phys.*, 2006, vol. 103 (5), pp. 819–29.
25. M.I. Ojovan and W.E. Lee: *J. Phys.: Condens. Matter*, 2006, vol. 18, pp. 11507–20.
26. M.I. Ojovan, K.P. Travis, and R.J. Hand: *J. Phys.: Condens. Matter*, 2007, vol. 19, 415107, 12 p.
27. M.I. Ojovan: *Adv. Condens. Matter Phys.*, 2008, vol. 2008, 817829, 23 p.
28. M. Sahimi: *Applications of Percolation Theory*, Taylor and Francis, London, UK, 1994.
29. M.B. Isichenko: *Rev. Mod. Phys.*, 1992, vol. 64, pp. 961–1043.
30. M.I. Ojovan: *J. Exp. Theor. Phys. Lett.*, 2004, vol. 79 (12), pp. 632–634.
31. R.P. Wool: *J. Polymer Sci. B*, 2008, vol. 46, pp. 2765–78.
32. V. Novotny: *Glass Int.*, 2010, vol. 32, pp. 21–25.
33. M. Ojovan, G. Möbus, J. Tsai, S. Cook, and G. Yang: *Proc. 12th Int. Conference on Environmental Remediation and Radioactive Waste Management ICEM2009*, Liverpool, NY, 2009, p. 10.
34. M.I. Ojovan: *Proc. WM'09 Conference*, Phoenix, AZ, 2008, p. 10.

35. G.M. Möbus, M.I. Ojovan, S. Cook, J. Tsai, and G. Yang: *J. Nucl. Mater.*, 2010, vol. 396, pp. 264–71.
36. N.R. Gribble, R. Short, E. Turner, and A.D. Riley: *Mater. Res. Soc. Symp. Proc.*, 2009, vol. 1193, pp. 283–90.
37. J.K. Bates, A.J.G. Ellison, J.W. Emery, and J.C. Hoh: *Mater. Res. Soc. Symp. Proc.*, 1996, vol. 412, pp. 57–64.
38. M.I. Ojovan, A.S. Pankov, W.E. Lee, and R.J. Hand: *Proc. WM'05 Conf.*, Tucson, AZ, 2005, p. 11.
39. F.A. Lifanov, M.I. Ojovan, S.V. Stefanovsky, and R. Burcl: *Proc. WM'03 Conf.*, Tucson, AZ, 2003, p. 9.
40. M.-J. Song: *Nucl. Eng. Int.*, 2003, February, pp. 22–26.
41. C.M. Jantzen, J.B. Pickett, and R.S. Richards: *Vitrification of Simulated Fernald K-65 Silo Waste at Low Temperatures*, WSRC-MS-97-00854, Rev. 1, 1997.
42. B.P. McGrail, D.H. Bacon, J.P. Icenhower, F.M. Mann, R.J. Schaef, H.T. Puigh, and S.V. Mattigod: *J. Noncryst. Solids*, 2001, vol. 298, pp. 95–111.
43. R. Alvarez: *Sci. Global Secur.*, 2005, vol. 13, pp. 43–86.
44. J.D. Vienna, P. Hrma, A. Jiricka, D.E. Smith, T.H. Lorier, R.L. Schulz, and I.A. Reamer: *Hanford Immobilized LAW Product Acceptance Testing: Tanks Focus Area Results*, Richland, WA, 2001.
45. J.A.C. Marples: *Glass Tech.*, 1988, vol. 29, pp. 230–47.
46. M.I. Ojovan, W.E. Lee, A.S. Barinov, I.V. Startceva, D.H. Bacon, B.P. McGrail, and J.D. Vienna: *Glass Tech.*, 2006, vol. 47 (2), pp. 48–55.
47. M.I. Ojovan and W.E. Lee: *Glass Tech.*, 2003, vol. 44, pp. 218–24.
48. J. Fleisch, W. Gruenewald, G. Roth, E. Schwaab, W. Tobie, and M. Weishaupt: *Proc. Int. Conf. WM'08*, Tucson, AZ, 2008, pp. 1–7.
49. IAEA TRS-291: *Design and Operation of Off-Gas Cleaning Systems at High Level Liquid Waste Conditioning Facilities*, IAEA, Vienna, Austria, 1988.
50. D.M. Strachan: *J. Nucl. Mater.*, 2001, vol. 298, pp. 69–77.
51. N.V. Krylova and P.P. Poluektov: *At. Energy*, 1995, vol. 78, pp. 93–98.
52. C.M. Jantzen, D.I. Kaplan, N.E. Bibler, D.K. Peeler, and M.J. Plodinec: *J. Nucl. Mater.*, 2008, vol. 378, pp. 244–56.
53. M.A. Rana and R.W. Douglas: *Phys. Chem. Glasses*, 1961, vol. 2 (6), pp. 179–205.
54. C.R. Das and R.W. Douglas: *Phys. Chem. Glasses*, 1967, vol. 8 (5), pp. 178–84.
55. R.H. Doremus: *J. Noncryst. Solids*, 1975, vol. 19, pp. 137–45.
56. A.A. Belyustin and M.M. Shultz: *Phys. Chem. Glasses*, 1983, vol. 9 (1), pp. 3–27.
57. B.P. McGrail, J.P. Isenhover, D.K. Shuh, P. Liu, J.G. Darab, D.R. Baer, S. Thevuthasen, V. Shutthanandan, M.H. Engelhard, C.H. Booth, and P. Nachimuthu: *J. Noncryst. Solids*, 2001, vol. 296, pp. 10–26.
58. M.I. Ojovan, A.S. Pankov, and W.E. Lee: *J. Nucl. Mater.*, 2006, vol. 358, pp. 57–68.
59. P. Aagaardand and H.C. Helgeson: *Am. J. Sci.*, 1982, vol. 282, pp. 237–85.
60. D.H. Bacon and B.P. McGrail: *Mater. Res. Soc. Symp.*, 2003, vol. 2 (1), pp. 1–9.
61. M.I. Ojovan, R.J. Hand, N.V. Ojovan, and W.E. Lee: *J. Nucl. Mater.*, 2005, vol. 340, pp. 12–24.
62. B.M.J. Smets and M.G.W. Tholen: *Phys. Chem. Glasses*, 1985, vol. 26, pp. 60–63.
63. W.L. Ebert: *Phys. Chem. Glasses*, 1993, vol. 34 (2), pp. 58–65.
64. P.K. Abraitis, F.R. Livens, J.E. Monteith, J.S. Small, D.P. Triverdi, D.J. Vaughan, and R.A. Wogelius: *Appl. Geochem.*, 2000, vol. 15, pp. 1399–416.
65. W.J. Weber, R.C. Ewing, C.A. Angell, G.W. Arnold, A.N. Cormack, J.M. Delaye, D.L. Griscom, L.W. Hobbs, A. Navrotsky, D.L. Price, A.M. Stoneham, and M.C. Weinberg: *J. Mater. Res.*, 1997, vol. 12, pp. 1946–78.
66. M.I. Ojovan and W.E. Lee: *J. Nucl. Mater.*, 2004, vol. 335, pp. 425–32.
67. L.R. Pederson and G.L. McVay: *J. Am. Ceram. Soc.*, 1983, vol. 66, pp. 863–867.
68. D.J. Wronkiewich: *Mater. Res. Symp. Proc.*, 1993, vol. 333, pp. 83–95.
69. P. Van Iseghem, E. Valcke, and A. Lodding: *J. Nucl. Mater.*, 2001, vol. 298, pp. 86–94.
70. D.M. Wellman, J.P. Isenhower, and W.J. Weber: *J. Nucl. Mater.*, 2005, vol. 340, pp. 149–62.
71. A. Abdelouas, K. Ferrand, B. Grambow, T. Mennecart, M. Fattahi, G. Blondiaux, and G. Houee-Levin: *Mater. Res. Soc. Symp. Proc.*, 2004, vol. 807, pp. 175–80.
72. M.I. Ojovan and W.E. Lee: *Proc. Int. Conf. WM'06*, Tucson, AZ, 2006, p. 13.